PSI TR-115

ADVANCED REENTRY AEROMECHANICS

FINAL REPORT

Period covered: 15 October 1973 - 30 November 1977

January 1978

Jointly Sponsored by

The Space and Missile Systems Organization

and

The Air Force Office of Scientific Research (AFSC)

Contract #F44620-74-C-0022

"Approved for Public Release; distribution unlimited"

PHYSICAL SCIENCES INC.
30 COMMERCE WAY, WOBURN, MASS. 01801

AIR FORCE OFFICE OF SCIENTIFIC RESEARCH (AFSC)
NOTICE OF TRANSMITTAL TO DDC
This technical report has been reviewed and is approved for public release IAW AFR 190-12 (7b).
Distribution is unlimited.
A. D. BLOSE
Technical Information Officer

UNCLASSIFIED

SECURITY CLASSIFICATION OF THIS PAGE (When Data Entered)

REPORT DOCUMENTATION PAGE

READ INSTRUCTIONS BEFORE COMPLETING FORM

1. REPORT NUMBER: AFOSR-TR-78-0607	2. GOVT ACCESSION NO.
3. RECIPIENT'S CATALOG NUMBER	
4. TITLE (and Subtitle): ADVANCED REENTRY AEROMECHANICS	5. TYPE OF REPORT & PERIOD COVERED: FINAL rept. 15 Oct 73 - 30 Nov 77
6. PERFORMING ORG. REPORT NUMBER: PSI-TR-115	
7. AUTHOR(s): M L FINSON, A N PIRRI, R E NEBOLSINE, G A SIMONS, R K S WU	8. CONTRACT OR GRANT NUMBER(s): F44620-74-C-0022
9. PERFORMING ORGANIZATION NAME AND ADDRESS: PHYSICAL SCIENCES INC, 30 COMMERCE WAY, WOBURN, MA 01801	10. PROGRAM ELEMENT, PROJECT, TASK AREA & WORK UNIT NUMBERS: 2307A1, AI, 61102F
11. CONTROLLING OFFICE NAME AND ADDRESS: AIR FORCE OFFICE OF SCIENTIFIC RESEARCH/NA, BLDG 410, BOLLING AIR FORCE BASE, D C 20332	12. REPORT DATE: Jan 78
	13. NUMBER OF PAGES: 33 35 pl
14. MONITORING AGENCY NAME & ADDRESS (if different from Controlling Office)	15. SECURITY CLASS. (of this report): UNCLASSIFIED
	15a. DECLASSIFICATION DOWNGRADING SCHEDULE

16. DISTRIBUTION STATEMENT (of this Report)

Approved for public release; distribution unlimited.

17. DISTRIBUTION STATEMENT (of the abstract entered in Block 20, if different from Report)

18. SUPPLEMENTARY NOTES

19. KEY WORDS (Continue on reverse side if necessary and identify by block number)

BOUNDARY LAYER TRANSITION
HYPERVELOCITY IMPACT
SURFACE EROSION
MULTIPHASE FLOW
MATERIALS TESTING

20. ABSTRACT (Continue on reverse side if necessary and identify by block number)

This report summarizes the results of a research program that addressed various aspects of hypersonic reentry vehicle design technology. A second-order turbulent closure model was extended to the prediction of boundary layer transition. The existing wind tunnel measurements of roughness-dominated nosetip transition were analyzed comprehensively. Three-dimensional laminar boundary layer computations were compared with data on the effect of angle of attack on conical transition, and a rather simple scaling law was derived. A technique was developed for simulating hypervelocity particle impact with a high power pulsed laser. The scaling requirements were derived, and a

DD FORM 1 JAN 73 1473 EDITION OF 1 NOV 65 IS OBSOLETE

UNCLASSIFIED

SECURITY CLASSIFICATION OF THIS PAGE (When Data Entered)

397 105

test program was conducted with a one joule ruby laser on a variety of surface materials. The validity of the simulation was demonstrated and many mass loss measurements were obtained. The behavior of ice crystals in shock layers was modeled using a two-layer melt removal analysis, a new dynamic fracture criterion for particle shattering, and an improved model for the deformation of the ice fragment cloud.

PSI TR-115

ADVANCED REENTRY AEROMECHANICS

FINAL REPORT

Period covered: 15 October 1973 - 30 November 1977

January 1978

Jointly Sponsored by

The Space and Missile Systems Organization

and

The Air Force Office of Scientific Research (AFSC)

Contract #F44620-74-C-0022

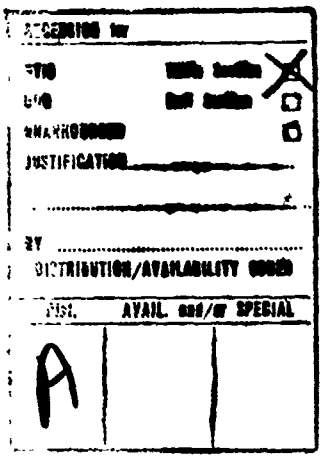

PHYSICAL SCIENCES INC.
30 Commerce Way
Woburn, MA 01801

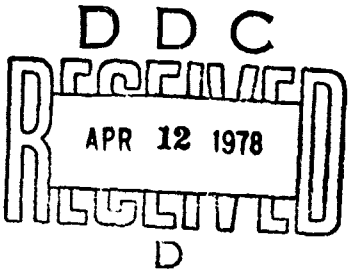

ABSTRACT

This report summarizes the results of a research program that addressed various aspects of hypersonic re-entry vehicle design technology. A second-order turbulent closure model was extended to the prediction of boundary layer transition. The existing wind tunnel measurements of roughness-dominated nosetip transition were analyzed comprehensively. Three-dimensional laminar boundary layer computations were compared with data on the effect of angle of attack on conical transition, and a rather simple scaling law was derived. A technique was developed for simulating hypervelocity particle impact with a high power pulsed laser. The scaling requirements were derived, and a test program was conducted with a one joule ruby laser on a variety of surface materials. The validity of the simulation was demonstrated and many mass loss measurements were obtained. The behavior of ice crystals in shock layers was modeled using a two-layer melt removal analysis, a new dynamic fracture criterion for particle shattering, and an improved model for the deformation of the ice fragment cloud.

ACKNOWLEDGEMENTS

Sponsorship Statement

Research jointly sponsored by the Space and Missile Systems Organization and the Air Force Office of Scientific Research (AFSC), United States Air Force, under Contract F44620-74-C-0022. The United States Government is authorized to reproduce and distribute reprints for governmental purposes notwithstanding and copyright notation hereon.

TABLE OF CONTENTS

LIST OF ILLUSTRATIONS

I. INTRODUCTION

This report summarizes the results of a research program, "Advanced Re-entry Aeromechanics", performed at Physical Sciences Inc. between October 1973 and November 1977. The program consisted of a number of tasks, addressing various aspects of hypersonic re-entry vehicle design technology, with much of the emphasis on nosetip design. The studies fall into two major categories, one addressing the prediction of boundary layer transition, and the other dealing with the erosive effects of ambient cloud particulate materials.

A substantial effort was devoted to the application of second order turbulent closure models for the prediction of boundary layer transition. Such techniques are inherently nonlinear and can generally be extended to relatively complicated situations such as hypersonic re-entry boundary layers. However, it remains to be demonstrated that the required closure approximations can be formulated in a physically well-founded manner. We found that reasonable results could be obtained in "by-pass" situations where the initial disturbance levels are large, due either to free-stream turbulence or surface roughness.

A critical analysis of the available wind tunnel data simulating nosetip boundary layer transition was performed. The most meaningful approach involved relating the Reynolds number based on momentum thickness at the transition location to a roughness Reynolds number, a wall temperature parameter, and to a term representing surface radius of curvature.

The effect of angle of attack on cone frustum transition fronts was also studied. By comparing appropriate three-dimensional laminar boundary layer computations with wind tunnel transition data, it was found that the observed shifts in the transition location involve a nearly constant value of

the momentum thickness Reynolds number, thus providing a relatively simple scaling law for estimating the effects of wind-fixed transition asymmetries on RV aerodynamics.

A most important result of the program was the development of a technique for simulating hypervelocity particle impact with a high power pulsed laser, affording a flexible, low cost screening method. Theoretical analyses were performed to determine the laser parameters required to simulate the impact of a given particle; the surface pressure history is matched, thus ensuring identical crater formation. Experiments were performed with a one joule Q-switched ruby laser on a variety of surface materials. The craters formed on ATJ-S graphite were examined by scanning electron microscopy and found to compare favorably with those created by actual particle impact. Mass loss data were obtained over a range of simulated particle impact conditions.

Finally, the interaction of ambient ice crystals with hypersonic shock layers was studied theoretically. A two-layer analysis was constructed to determine melt layer removal from the ice due to heating within the shock layer, and maps of the resulting impact energy were obtained. The mechanical fragmentation of ice crystals due to the sudden pressure loadings was described with a new dynamic fracture criterion, which predicts that the crystals generally shatter into a cloud of much smaller particles. We modeled the subsequent deformation and slowdown of the fragment cloud, and obtained results that also prove useful for the study of liquid drop deformation.

II. BOUNDARY LAYER TRANSITION STUDIES

A. The Application of Second-Order Closure Models To Boundary Layer Transition (Refs. 1 - 3)

Boundary layer transition has an important effect on re-entry vehicle nosetip shape change and recession. A significant study effort has been devoted to extending second-order closure techniques, which have become quite useful for studying turbulent flows, to the prediction of transition. One obvious motivation stems from the fact that second-order models are non-linear, and hence may provide useful results in the later stages of transition. On the other hand, the transition process is enormously complex, and it must be demonstrated that the required closure approximations can be made in a manner that is physically sound for transition regimes. One would hardly expect the second-order models to reproduce linear stability theory. However, it might be anticipated that the method would have some real validity in "by-pass" situations, where transition is triggered by relatively high levels of initial fluctuations, introduced by either free-stream turbulence or surface roughness.

Our studies utilized a "five-equation" model; the dependent fluctuating quantities are the three components of the fluctuating kinetic energy $\overline{u'^2}$, $\overline{v'^2}$, $\overline{w'^2}$, the Reynolds stress $\overline{u'v'}$, and either the dissipation rate Φ or the length scale Λ. With this set, closure is not required for the production terms except in the length scale equation. There is also little difficulty with molecular diffusion terms, which are exact, or with the turbulent diffusion terms, which are not particularly important during transition. For the dissipation terms, it is important to include low Reynolds number effects, which can be done by relying on exact solutions for the zero Reynolds number limit. Perhaps most crucial is the treatment of the pressure fluctuation terms, which describe the transfer of energy between components. The

existing turbulent closure expressions for these terms result in an overly rapid generation of turbulent energy in transition predictions. Modifications were developed to account for the fact that the length scales are larger than the boundary layer thickness during transition, enabling more realistic computation of transition. However, additional study would be desirable to put the closure of these pressure fluctuation terms on a really sound basis.

Figure 1 shows a comparison of calculations, based on the closure model, with data on the effect of free-stream turbulence on transition on flat plates in low speed flows. As discussed in more detail in Refs. 1 - 3, the comparison should be qualified by the uncertain nature of the free-stream turbulence in the experiments. In most wind tunnels, the free-stream fluctuations are largely acoustic rather than vortical, whereas the closure treatment accounts only for the latter type.

The effect of distributed surface roughness on transition was also examined. To this end, it was necessary to describe the manner by which roughness elements disturb the boundary layer. Attached flow was assumed, and distributed source or sink terms were developed to apply at heights below the tops of the elements. The primary terms were a sink term in the mean momentum equation, accounting for drag on the elements, and a source term in the kinetic energy equation, which represents the fluctuations created by the roughness. Figure 2 shows the resulting calculations for transition, compared to data on flat plates roughened with sandpaper. The figure indicates a reasonable agreement, if the effects of free-stream turbulence are included. Below a roughness Reynolds number of about 200, we predict that the roughness should be ineffective at tripping the boundary layer.

B. An Analysis of Nosetip Transition Data (Ref. 4)

This task involved an independent, critical evaluation of the available ground test data on nosetip boundary layer transition, and of the transition

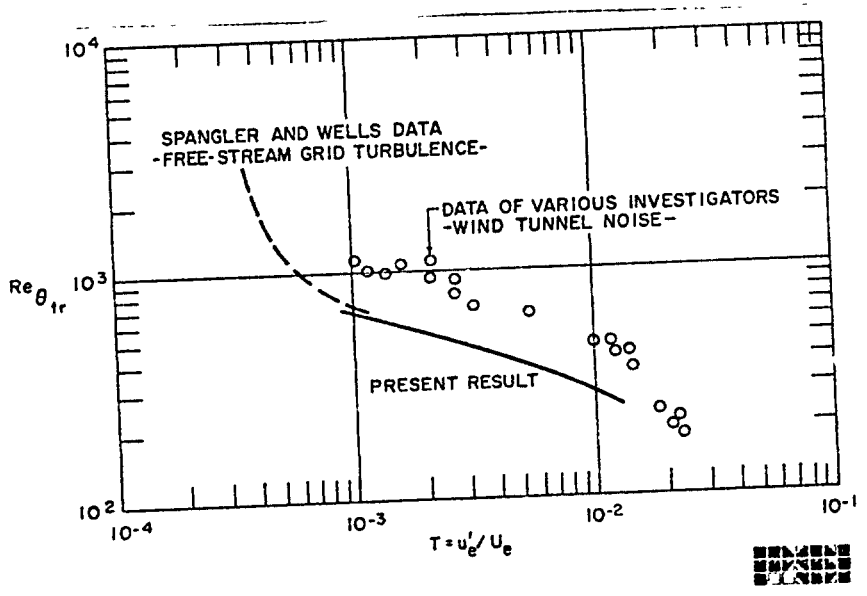

Fig. 1 Comparison of experimental results and the calculations based on second-order closure model for the effect of free-stream turbulence on boundary layer transition on flat plates.

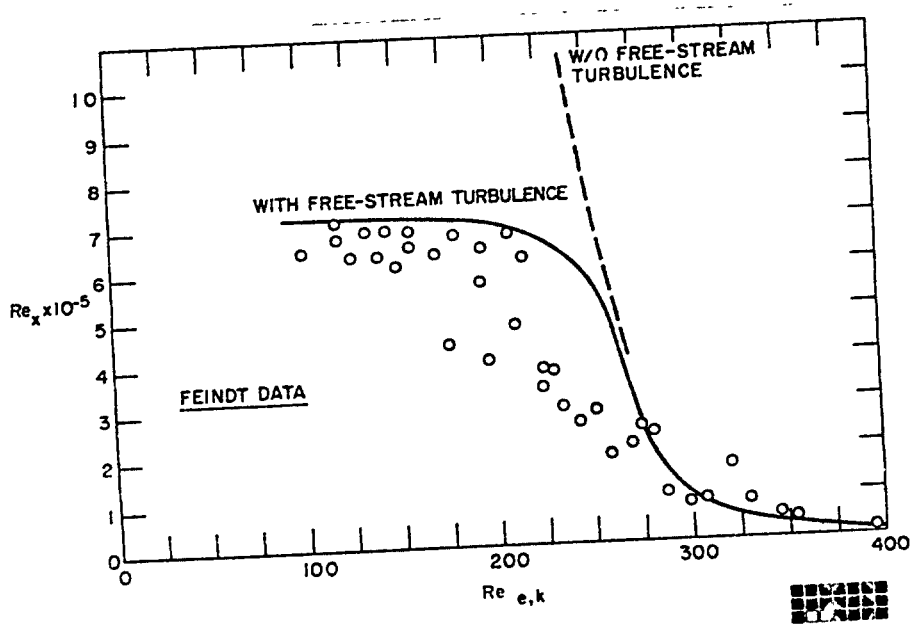

Fig. 2 Comparison of experimental results and calculations based on second-order closure model for the effect of distributed surface roughness on boundary layer transition on flat plates.

criteria used for nosetip design. Numerous correlations have been developed by various investigators, and the primary objective of this study was to evaluate the behavior of transition as a function of parameters that are thought to be physically well-founded. In addition, we evaluated the data base and recommended additional tests to resolve uncertain trends.

For flight applications, nosetip transition is normally controlled by the inherent surface roughness. After listing nearly all of the imaginable non-dimensional parameters, four or five were considered to be most relevant to nosetip transition. As have most other investigators, we concluded that the Reynolds number based on edge conditions and momentum thickness, $Re_{e,\theta} = \rho_e u_e \theta/\mu_e$, is the most appropriate measure of the transition location. The roughness Reynolds number $Re_{k,k} = \rho_k u_k k/\mu_k$, involving roughness height k and conditions at the top of the roughness, was used an an independent parameter, although one could have selected k/θ, which is related to $Re_{k,k}$. The well-known wall temperature effect is described by T_w/T_e, and there may also be a dependence on θ/R_c (R_c = surface radius of curvature), which may be due to centrifugal acceleration or pressure gradient.

The wall temperature effect was found to be most easily described by modifying $Re_{e,\theta}$ to base it on fluid properties in the middle of the boundary layer. For convenience we used the geometrical mean of the edge and wall values of the viscosity $\nu_m = (\nu_w \nu_e)^{1/2}$. The existing data, primarily that obtained in the PANT program, suggest a curvature effect. Figure 3 shows the correlation of the PANT data[5] that resulted from this study. Except for some relatively low roughness cases, where free-stream turbulence can be important, and a few cases with extremely large roughness, a successful correlation is obtained. Data from other studies, which are not included in this figure for sake of clarity, are consistent with the data shown. It should be noted that the curvature term rather nicely accounts for the "onset"

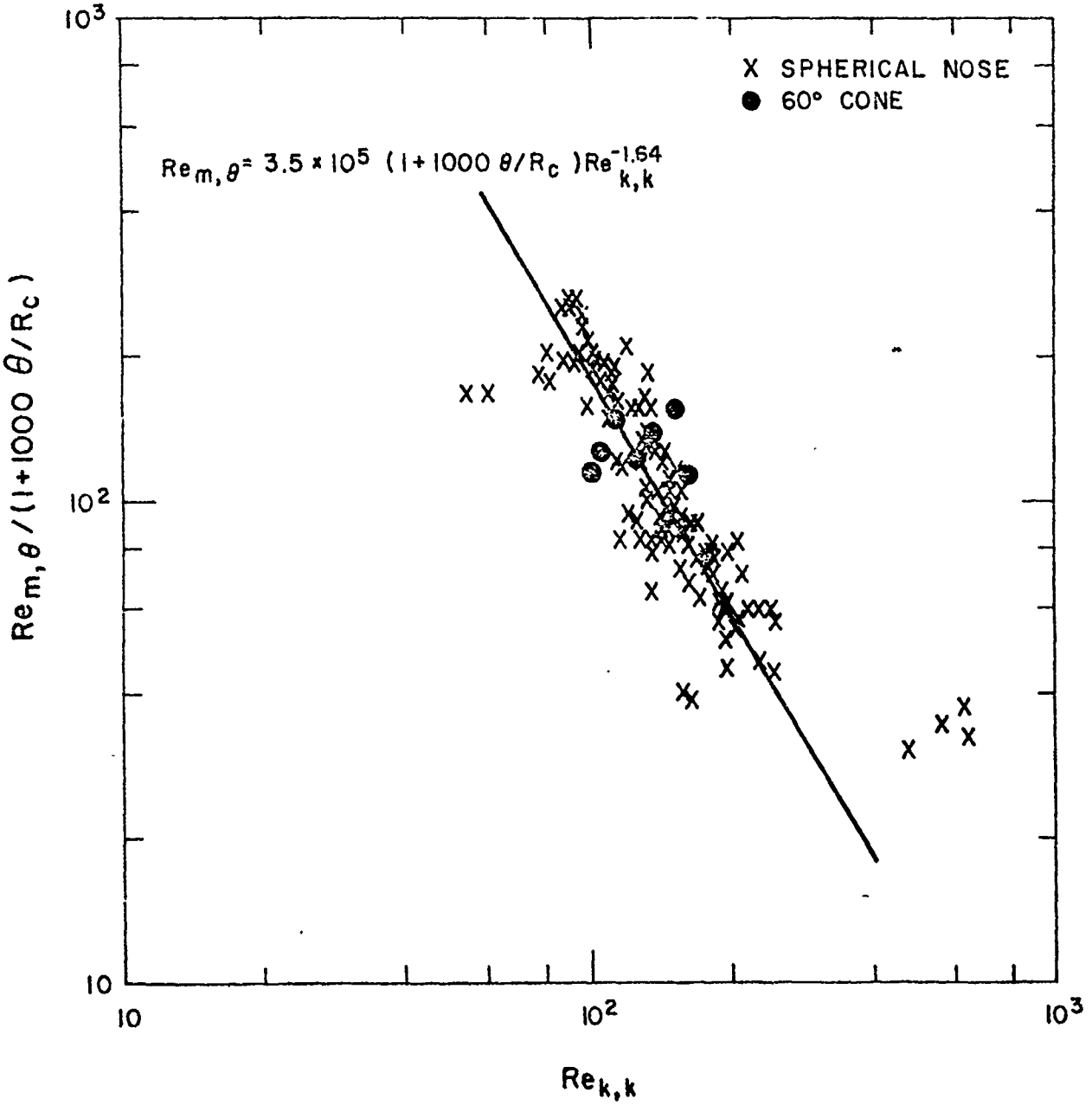

Fig. 3 Correlation of wind tunnel data[5] simulating reentry nosetip transition.

phenomenon, which required a second criterion in the PANT study. Another unique feature of this analysis was the use of the roughness model mentioned in the previous section to compute the laminar boundary layer momentum thickness, rather than using smooth wall computations. According to our results, roughness increases the boundary layer thickness for $k/\theta \geq 4$.

We also performed some algebraic manipulations to express the various existing nosetip transition correlations in common variables, to determine the differences between them over the expected range of conditions where flight predictions would be required. For all practical purposes, it was found that the correlation shown in Fig. 3 yields predictions quite similar to those given by the PANT[6] and van Driest[7] correlations. However, Bishop's criterion[8] predicts a significantly larger transition Reynolds numbers at high Mach numbers and small roughness heights..

There are several areas where the additional ground test data are desirable. There is an important practical question of properly defining the roughness height k for actual nosetip materials, and wind tunnel tests with surfaces that accurately reproduce the roughness character of graphite and composites are indicated. There is also a lack of wind tunnel data on the combined effects of roughness and blowing. Finally, better wind tunnel data are needed for very small and large roughness heights, and for non-hemispherical noses.

C. Analysis of Wind-Fixed Transition Asymmetries (Ref. 9)

A non-zero angle of attack introduces asymmetries in the location of boundary layer transition on the conical frustum of a re-entry vehicle, resulting in significant changes in aerodynamic characteristics. In this study we developed a correlation or scaling law for the variation in the frustum transition location with angle of attack, by interpreting the available wind tunnel results in terms of local boundary layer properties.

To obtain the desired laminar boundary layer solutions, we used the small cross-flow approximations, following Fannelop,[10] although with a finite-difference technique rather than the similarity approximations of Fannelop. The inviscid properties were obtained from a 3-D program "3DSAP" developed by the General Electric Company. The resulting calculations show cross-flow within the boundary layer (relative to edge streamlines) to be quite small at angles of attack in the range of interest ($1 - 2^{\circ}$), so that "equivalent cone" calculations would have been acceptable.

There are three characteristics of the 3-D boundary layer solutions that are particularly noteworthy. First, angle of attack causes the boundary layer to thicken considerably on the lee side, which may explain why transition often moves forward there. Second, with a blunt nose, the entropy layer causes $Re_{e,\theta}$ ($= \rho_e u_e \theta/\mu_e$) to be less than on a sharp cone of the same size, even at no angle of attack. Third, entropy swallowing is accelerated on the windward side of blunt cones. The "reversal" that is occasionally observed on blunted cones - forward motion of transition on the windward side - can be interpreted as a combination of the second and third effects.

To analyze the available wind tunnel data in a quantitative manner, we studied the ratio of the Reynolds number based on edge properties and momentum thickness at angle of attack to that at no angle of attack, $(Re_{e,\theta})_{\alpha}/(Re_{e,\theta})_{\alpha=0}$. Hopefully, use of this ratio will remove the complicated trends with wall temperature, free-stream noise, etc., that have been widely observed at $\alpha=0$. To measure the effect of angle of attack, the inviscid cross-flow angle at the 90° side meridian (W_e/U_e) was used. Figure 4 shows the resulting compilation of wind tunnel data. Transition apparently tends to occur at approximately a constant value of $Re_{e,\theta}$. On the lee side, transition may shift forward substantially, but it actually occurs at slightly higher values of $Re_{e,\theta}$. Note that this result does not indicate evidence for any destabilizing effect on the lee side, as has been suggested often in the

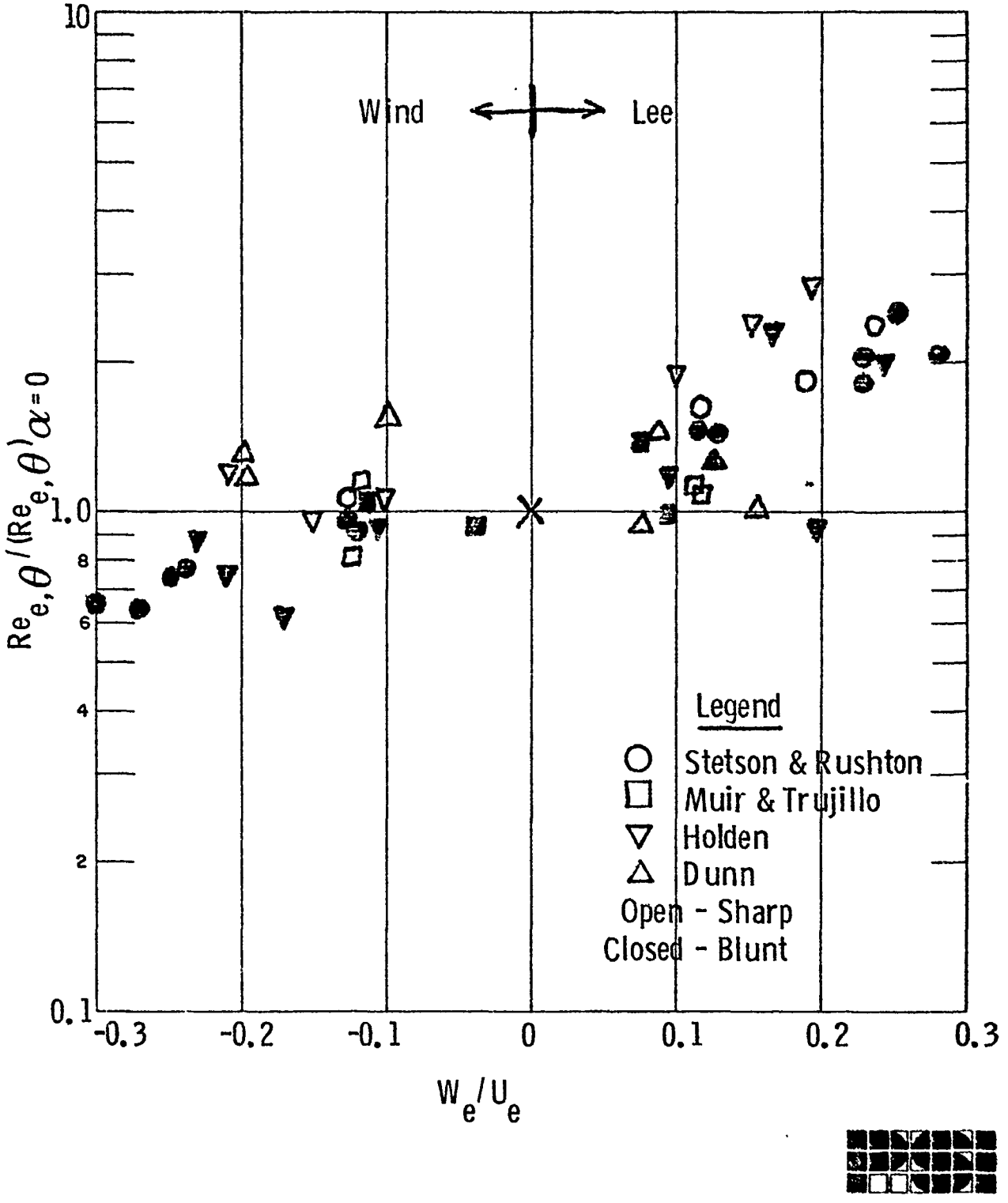

Fig. 4 Analysis of the effect of angle of attack on cone transition Reynolds numbers.

literature. The data scatter in the figure can be the result of a number of factors, including natural fluctuations in the transition location, lack of a perfect correlation technique, or limited spatial resolution in the experiments. Nevertheless, a rather straightforward scaling law is evident for the vehicle designer to use in assessing vehicle aerodynamic characteristics.

III. HYPERVELOCITY EROSION STUDIES

A. Laser Simulation of Hypervelocity Impact (Refs. 11 - 13)

One of the most interesting and significant parts of the program was the development of a technique for simulating the hypervelocity impact of ambient water or ice particles on re-entry vehicles with a high power pulsed laser. If properly scaled, the laser pulse will produce craters comparable to those caused by particle impact. Compared to particle acceleration techniques or ballistic range tests, the laser simulation provides a flexible, low cost method for assessing erosion rates or screening heatshield materials.

A fairly extensive theoretical analysis was performed to determine the required laser parameters for simulating impact of a given particle.[11] A highly focused laser beam causes rapid evaporation of surface material, and energy absorption in the evaporated material produces plasma breakdown and generates a high pressure. The primary requirements for laser simulation of particle impact are that the particle impact pressure should be matched, the laser spot size should match the projectile diameter, and that the laser pulse duration should equal the appropriate particle/surface interaction time. The particle-generated impact pressure was computed from the one-dimensional shock model of Gehring,[14] along with Hugoniot curves for the particle and target material. The particle interaction time, which is much less than the crater formation time, was taken from the results of Eichelberger and Gehring.[15] A simplified theory for the interaction of a highly focused pulsed laser beam with a surface was developed to obtain the laser-induced surface pressures, accounting for the laser energy deposition in the plasma created. Details of the analysis may be found in Ref. 11.

Figure 5 presents the resulting laser requirements for simulating hypervelocity impact with a 0.7 μm laser, for the case of water droplets

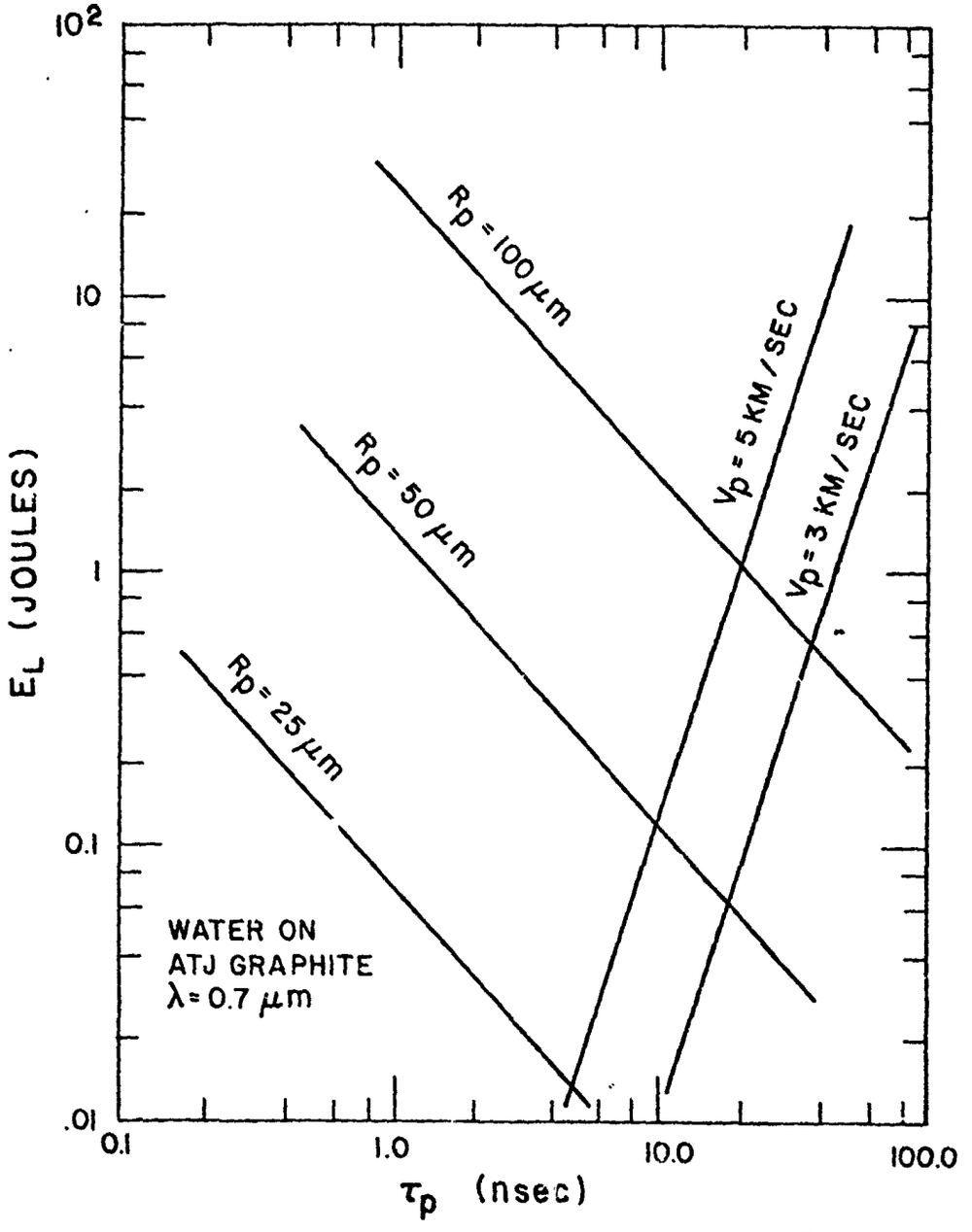

Fig. 5 Laser scaling requirements for hypervelocity impact simulation with a 0.7μ laser.

impacting graphite. It can be seen that pulse energies of ≤ 1 joule and pulse times of ~ 10 nsec are sufficient to simulate impact velocities typical of re-entry conditions.

An experimental program was then undertaken to perform the actual laser simulations,[12,13] A Q-switched ruby laser with a pulse energy of 1 joule and pulse duration of 40 nsec was used. This permitted simulation of particles up to about 100 μm in size, although larger particles could be simulated with a larger laser. When focused down to 100 μm, the irradiance is $\sim 10^{11}$ watts/cm^2. This high flux produces the impact pressures, 10^{11} - 10^{12} dynes/cm^2, that occur in hypervelocity impact. The experiments were done in a Lucite vacuum chamber at a pressure of 100 - 300 μm of Hg, to prohibit plasma generation and formation of a laser-supported detonation wave in the ambient gas above the surface. The laser output was monitored with a calorimeter and silicon photodiodes. Tests were performed on brittle materials such as ATJ-S graphite and glass, and on ductile materials such as aluminum and copper. Backface interferometry was used to check the induced shock duration and strength.[13] Scanning electron micrographs were made of the laser produced craters, and many mass loss measurements were obtained.

Figure 6 is an example of a scanning electron micrograph of a laser produced crater, along with one of a particle impact crater. Even though there is a factor of six difference in scale, the craters are qualitatively very similar. Note the shelf on the edge of the crater and the deeper central region in each crater. The grain structure is more noticeable in the laser-produced crater due to the smaller crater size. Similar crater morphology was pursued in aluminum and copper, again demonstrating great similarity to craters produced by actual impact.

A number of tests were performed in ATJ-S graphite to obtain mass loss measurements at various equivalent particle conditions. Figure 7

LASER PRODUCED CRATER IN GRAPHITE

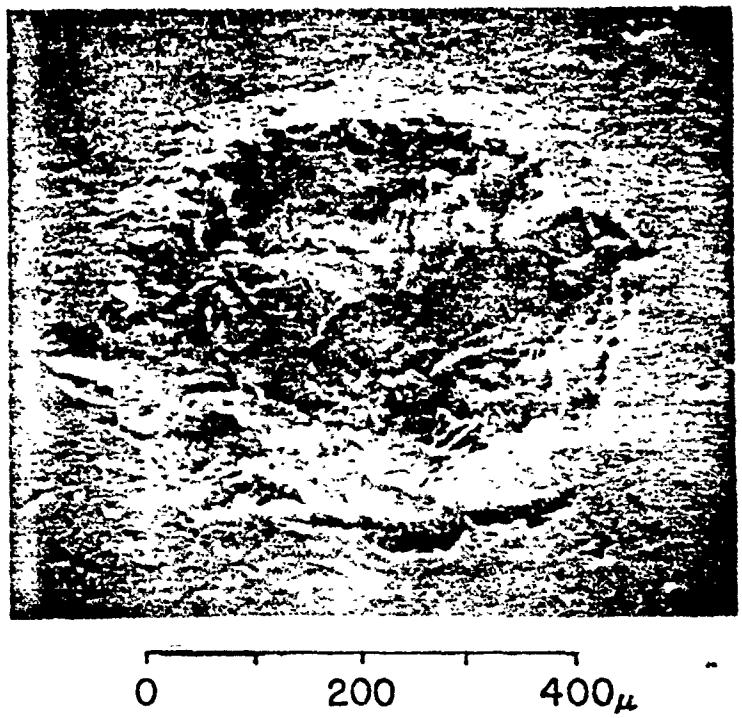

Fig. 6a Laser Produced Crater in Graphite

GLASS PARTICLE CRATER IN GRAPHITE[16]

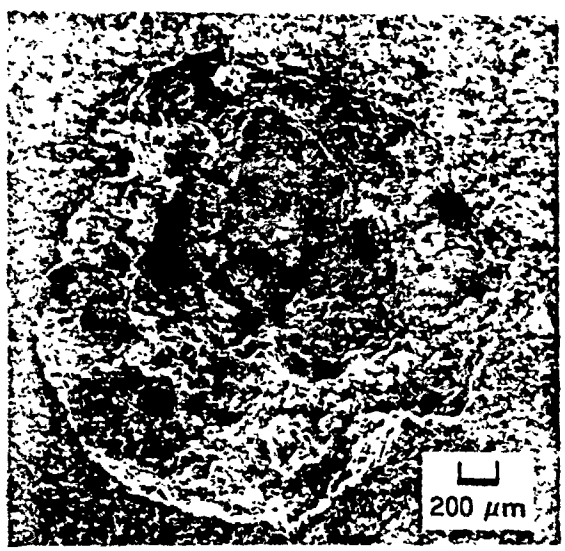

Fig. 6b Glass Particle Crater in Graphite

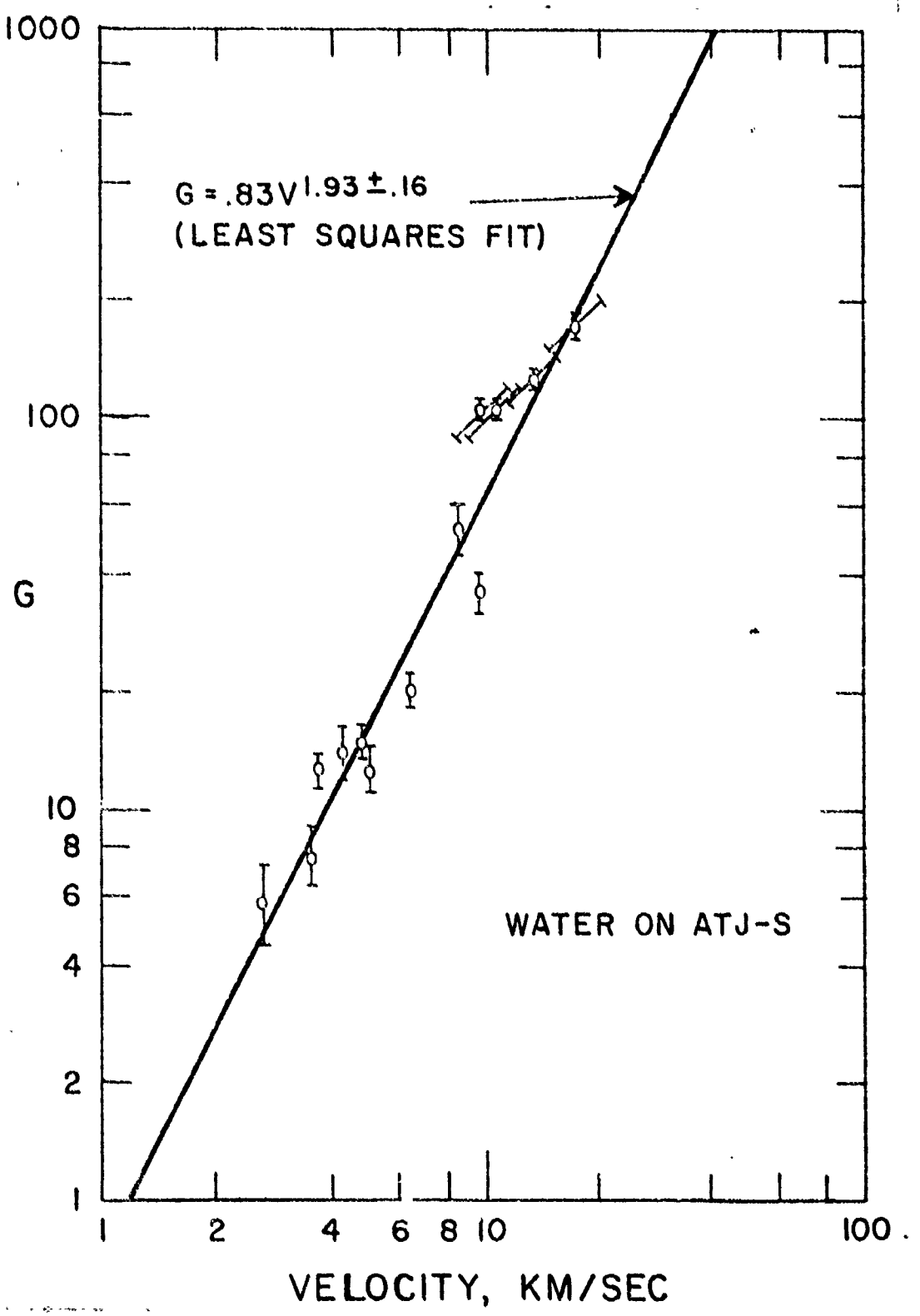

Fig. 7 Mass loss ratio vs. velocity, as derived from laser hypervelocity impact simulation measurements on ATJ-S graphite.

shows the results for a simulation of water droplets impacting ATJ-S; the quantity G is the ratio of the measured mass loss to the mass of the simulated impacting particle. These measurements involved producing 30 - 60 craters on each sample, at separate non-overlapping locations, to obtain an easily measurable mass loss. Note that the best fit to the data indicates that the mass loss is nearly proportional to the kinetic energy of the simulated particles, which is in good agreement with published hypervelocity particle impact data. Some tests were also conducted in which the surface was subjected to multiple overlapping cratering, simulating flight through an extensive cloud. This is straightforward since the ruby laser system could be pulsed every few seconds. Interestingly, approximately a 50% enhancement in mass loss was found on the predamaged surface compared to the virgin material.

B. Ice Crystal/Shock Layer Studies (Refs. 1, 17 - 18)

An important consideration in assessing the re-entry vehicle erosion caused by ambient particulates is the behavior of the particles in the shock layer of the body. Although the response of water droplets and solid particles had received detailed experimental and theoretical study, little attention had been given to the ice crystals that can represent the major portion of high altitude moisture in clouds. Accordingly, we addressed two major topics: 1) the mass loss due to heating, which requires a treatment of the heat transfer to an ablating ice particle in a hypersonic shock layer;[1] and 2) an investigation of the possible breakup mechanisms of typical ice crystals as they are subjected to mechanical and thermal stresses traversing the bow shock wave.[17,18]

When an ice crystal traverses the shock layer of a hypersonic vehicle, the aerodynamic heat transfer and shear forces cause the ice to melt and form a flowing liquid layer. The approach that was used to model the melt

layer removal is similar to that developed to calculate the heat transfer to glassy ablators. Due to the relatively high viscosity of water, the velocity of the liquid layer will be small compared to the gas velocity. This allows neglect of inertial effects in the melt layer and of any effect of the liquid motion on the gas boundary layer. The resulting two-layer problem can be solved in a relatively straightforward manner. The heat transfer from the air boundary layer (which corresponds to a doubly-shocked environment), and the corresponding shear stress are characterized in terms of an unknown mass injection rate (by vaporization of the liquid layer). The liquid layer equations are then solved with this heat transfer and shear as boundary conditions, and the resultant mass flux rates from liquid to vapor and from solid to liquid are obtained from the solution. Finally, the particle trajectory is integrated across the shock layer.

Perhaps the most relevant presentation of the ice crystal heating and trajectory calculations is the particle kinetic energy at impact. This is shown in Fig. 8, as a fraction of the initial kinetic energy, versus initial ice crystal diameter at the stagnation point of a body with a one inch nose radius. A previous calculation by N. Jaffe (Aerotherm /Acurex Corp.) neglected the effect of melting on the heat transfer.[17] The curve with $\mu = \infty$ represents the situation where the melt layer cannot flow off the ice crystal. The results indicate that ice crystal erosion will be minimal for crystal sizes less than about 20 μm.

The other major issue in the shock layer response of ice crystals is the possibility of mechanical shattering and deformation. The doubly-shocked pressures can easily exceed the standard quoted values for the ultimate strength of single crystals, although such values apply only at relatively low rates of load application. Accordingly, a dynamic fracture criterion was developed, which considers a Fourier component of the applied stress wave and applies the yield criterion to each component. The analysis, which is

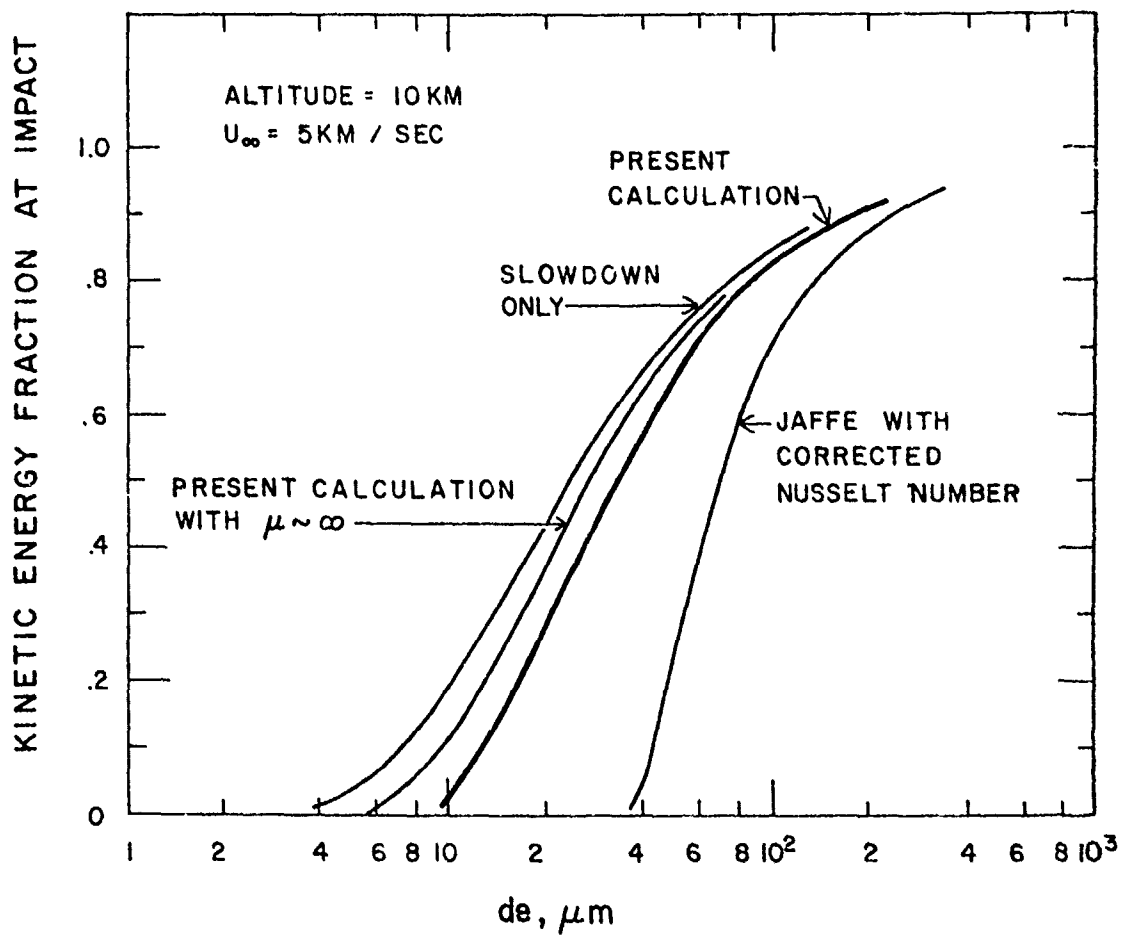

Fig. 8 Computed results for the reduction of ice crystal impact energy due to slowdown and melting in the shock layer of a reentry body with a one inch nose radius.

described in detail in Ref. 18, indicates that a wide range of wavelengths is capable of shattering typical crystals, and that the crystal will usually shatter into a cloud of small fragments.

It is further shown in Ref. 18 that the resulting fragment cloud will behave as an incompressible fluid without surface tension. Thus the ice crystal breakup is basically insensitive to the actual shattering process and the primary effect of interest is the lateral spreading of the fragment cloud, increasing the deceleration within the shock layer. A simplified theory for the cloud deformation, which accounts more accurately for the coupled effects of deformation and deceleration than has been done in previous liquid drop studies, was developed and is presented in Ref. 19. Figure 9 illustrates the importance of this increased slowdown of the fractured ice crystal cloud on the surface impact energy.

Fig. 9 Computed results for the reduction of ice crystal impact energy due to ice crystal fragmentation and subsequent deformation of the fragment cloud.

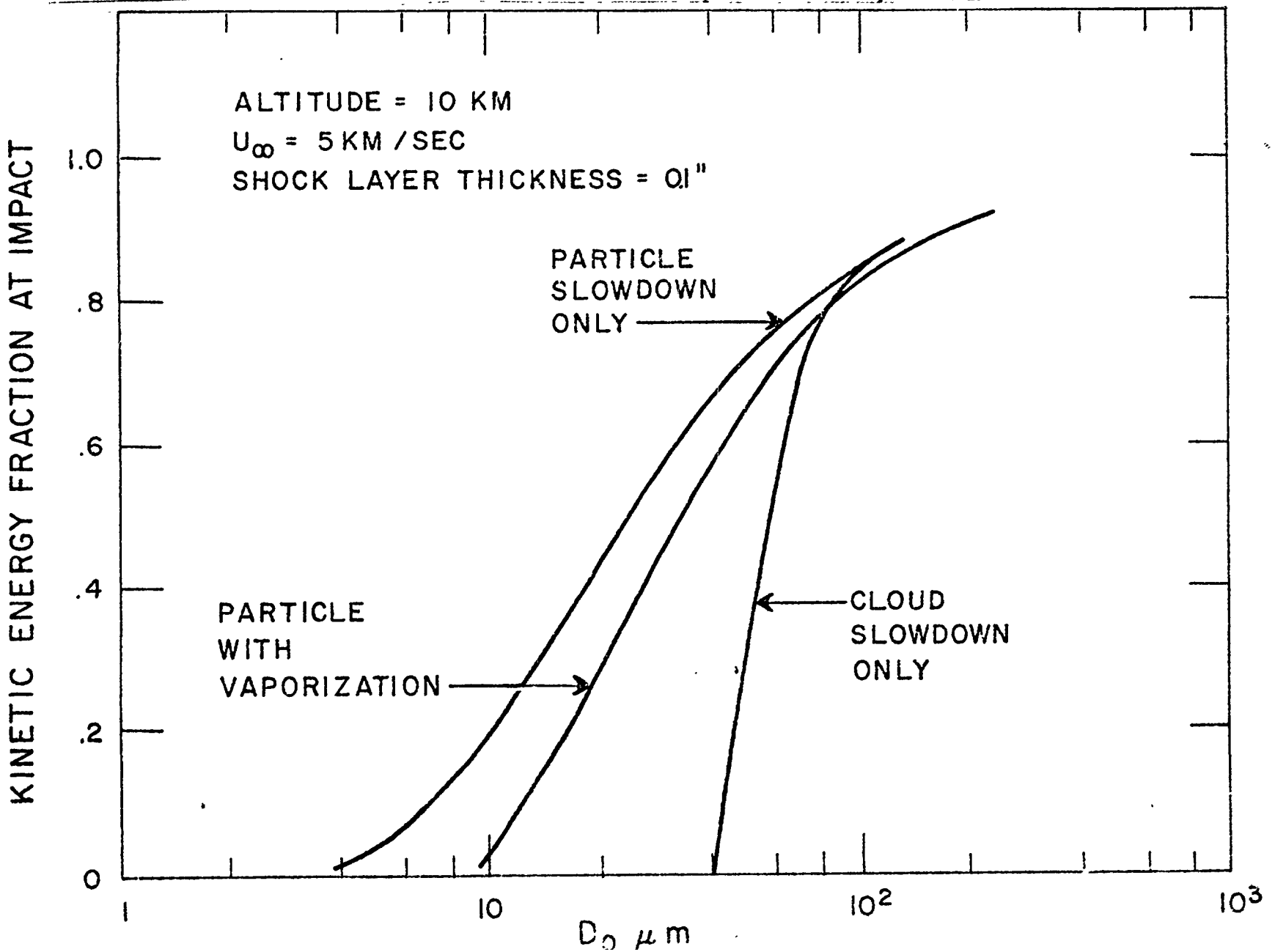

IV. LIST OF PUBLICATIONS

1. Finson, M. L., Lewis, P. F., Wu, P. K. S., Teare, J. D., Pirri, A. N. and Nebolsine, P. E., "Advanced reentry Aeromechanics, Interim Scientific Report", Physical Sciences Inc., PSI TR-10, August 30, 1974.

2. Finson, M. L., "A Reynolds Stress Model for Boundary Layer Transition with Application to Rough Surfaces", Physical Sciences Inc., TR-34, SAMSO-TR-76-0322 (1975).

3. Nebolsine, P. E., "Laser Simulation of Hypervelocity Impact", AIAA Paper 76-52, January 1976, PSI SR-5.

4. Simons, G. A., "Liquid Drop Acceleration and Deformation", AIAA J., 14, 2, 278-280, February 1976. Also PSI TR-22, April 1975.

5. Simons, G. A., "Aerodynamic Shattering of Ice Crystals in Hypersonic Flight", AIAA J., 14, 11, 1563-1570, November 1976. Also PSI TR-22, April 1975.

6. Finson, M. L., "An Analysis of Nosetip Boundary Layer Transition Data", PSI TR-52, August 1976.

7. Pirri, A. N., "Theory for Laser Simulation of Hypervelocity Impact", Phys. of Fluids 20, 221 (1977).

8. Nebolsine, P. E., "Laser Simulation of Hypervelocity Impact", PSI TR-92, May 1977.

9. Finson, M. L., "On the Application of Second-Order Closure Models to Boundary Layer Transition", AGARD conference on Laminar-Turbulent Transition, AGARD-CP-224, May, 1977.

10. Finson, M. L., "Boundary Layer Transition on Cones at Angle of Attack", in preparation.

V. REFERENCES

1. Finson, M. L., Lewis, P. F., Wu, P. K. S., Teare, J. D., Pirri, A. N. and Nebolsine, P. E., "Advanced Reentry Aeromechanics, Interim Scientific Report", Physical Sciences Inc., PSI TR-10, August 30, 1974.

2. Finson, M. L., "A Reynolds Stress Model for Boundary Layer Transition with Application to Rough Surfaces", Physical Sciences Inc., TR-34, SAMSO-TR-76-0322 (1975).

3. Finson, M. L. "On the Application of Second-Order Closure Models to Boundary Layer Transition", AGARD conference on Laminar-Turbulent Transition, AGARD-CP-224, May, 1977.

4. Finson, M. L., "An Analysis of Nosetip Boundary Layer Transition Data", PSI TR-52, August 1976.

5. Wool, M. R., "Final Summary Report Passive Nosetip Technology (PANT) Program", Aerotherm Report 75-159, SAMSO-TR-75-250 (1975).

6. Anderson, A. D., "Boundary Layer Transition on Nosetips with Rough Surfaces", in Appendix A of "Passive Nosetip Technology (PANT) Program, Interim Report", Aerotherm Report 74-100, SAMSO-TR-74-86, Vol. X (1975).

7. van Driest, E. R., Blumer, C. B. and Wells, Jr., C. S., "Boundary-Layer Transition on Blunt Bodies - Effect of Roughness", AIAA J. 5, 1913-1915 (1967). Also van Driest, E. R., "Evaluation of PANT Transition-Roughness Data and Transition Criterion", Private Communication (1975).

8. Bishop, W. M., "Transition Induced by Distributed Roughness on Blunt Bodies in Supersonic Flow", Aerospace Corp. TR-0077 (2550-15)-1, SAMSO-TR-76-146, October 1976.

9. Finson, M. L., "Boundary Layer Transition on Cones at Angle of Attack", in preparation.

10. Fannelop, T. K., "A Method of Solving the Three-Dimensional Laminar Boundary Layer Equations with Application to a Lifting Re-Entry Body", AIAA J. Vol. 6, pp 1075-1084, 1968.

11. Pirri, A. N., "Theory for Laser Simulation of Hypervelocity Impact", Phys. of Fluids 20, 221 (1977).

12. Nebolsine, P. E., "Laser Simulation of Hypervelocity Impact", AIAA Paper 76-52, January 1976, PSI SR-5.

13. Nebolsine, P. E., "Laser Simulation of Hypervelocity Impact", PSI TR-92, May 1977.

14. Gehring, J. W., "Theory of Impact on Thin Targets and Shields and Correlation with Experiment", High-Velocity Impact Phenomena, R. Kinslow, ed., Academic Press, New York (1970).

15. Eichelberger, R. J. and Gehring, J. W., "Effects of Meteoroid Impacts on Space Vehicles", American Rocket Society Journal, 32, No. 10, 1583 (1962).

16. Jaffe, N. A., "Droplet Dynamics in a Hypersonic Shock Layer", AIAA Journal, Vol. 11, No. 11, November 1973, P 1562.

17. Simons, G. A., "Aerodynamic Shattering Of Ice Crystals in Hypersonic Flight", AIAA J., 14, 11, 1563-1570, November 1976. Also PSI TR-22, April 1975.

18. Simons, G. A., "Liquid Drop Acceleration and Deformation", AIAA J., 14, 2, 278-280, February 1976. Also PSI TR-22, April 1975.